

Intermediate Strain-Rate Loading – Techniques and Applications

L. C. Chhabildas, W. D. Reinhart, K. G. Holland
 Sandia National Laboratories, Albuquerque, NM 87185

A new test methodology is described which allows access to loading rates that lie between split Hopkinson bar and shock-loading techniques. Gas gun experiments combined with velocity interferometry techniques have been used to experimentally determine the intermediate strain-rate loading behavior of Coors AD995 alumina and Cercom silicon-carbide rods. Graded-density materials have been used as impactors; thereby eliminating the tension states generated by the radial stress components during the loading phase. Results of these experiments demonstrate that the time-dependent stress pulse generated during impact allows an efficient transition from the initial uniaxial strain loading to a uniaxial stress state as the stress pulse propagates through the rod. This allows access to intermediate loading rates over 5×10^3 /s to a few times 10^4 /s.

1. Introduction

A new test methodology is described which allows access to loading rates that lie between split Hopkinson bar and shock-loading techniques. Traditional split Hopkinson bar techniques allow measurements on the failure stress of the material at loading rates up to 10^3 /s, where the definition of the failure stress is the yield strength of the material determined under uniaxial-stress loading. In contrast, plate impact techniques introduce uniaxial strain states at loading rates of 10^5 /s or higher. At these very high strain rates the failure stress is defined as the stress at which the material transitions from elastic deformation to plastic deformation normally defined as the Hugoniot elastic limit of the material. The experimental test methodology in each case prevents access to loading rates of the order of 10^4 /s. It is the purpose of this paper to report a new test methodology that allows access to loading rates of 10^4 /s. This is referred to, in this study, as intermediate strain rate loading.

A single-stage compressed gas gun combined with velocity interferometry techniques [1] was used to experimentally determine the loading behavior of ceramic rods about 19 mm in diameter by 74 mm in length. Graded-density materials [2,3] were used to impact both bare and sleeved ceramic rods [4-6] while the velocity interferometer [7] was used to monitor the axial velocity of the free end of the rods.

Results of these experiments demonstrate unique features of this novel test methodology:

- (a) A time-dependent stress pulse generated resulting from graded-density impact allows a smooth and efficient transition from the initial uniaxial strain loading to a uniaxial stress state as the stress pulse propagates through the rod, and
- (b) intermediate loading rates of 10^4 /s obtained in this configuration lie in a region which is not achieved easily by either split Hopkinson bar or shock-loading techniques.

In this paper, only the results of experiments conducted on Cercom silicon carbide rods are reported. Results of Coors AD995 alumina rod experiments are published elsewhere [4,5].

* Sandia is a multiprogram laboratory operated by Sandia Corporation, a Lockheed Martin Company, for the United States Department of Energy under Contract DE-AC04-94AL85000.

2. Experimental Technique

These experiments were performed on a 64 mm diameter, smooth-bore, single-stage, compressed gas gun which is capable of achieving a maximum velocity of about 1.6 km/s. Three electrically shorting pins were used to measure the velocity of the projectile at impact. Four similar pins were mounted flush to the impact plane and used to monitor the planarity of impact. Projectile velocity was measured with an accuracy of about 0.5% and the deviation from planarity of impact was about a milliradian. The graded-density impactor assembly is fabricated by bonding a series of thin plates in order of increasing shock impedance from the impact surface. The series of layered materials used in these studies were TPX-plastic, aluminum, titanium, and 4340 steel. The thickness of each layer is controlled to tailor the (time-dependent) input stress pulse into the silicon carbide rod. The exact dimensions of each material assembly is given in Table 1. This layered material assembly is used as facing on an aluminum projectile which is accelerated on a gas gun to velocities from 340 m/s to 620 km/s prior to impact. This provides a time-dependent loading at the impact interface from about 6.56 GPa to ~ 15 GPa, which is beyond the Hugoniot Elastic Limit for the material [8-10]. The experimental target assemblies consisted of either a bare or a sleeved silicon carbide rod ~ 19 mm in diameter. The length of the rods in this study were nominally 74 mm and 4340 steel was chosen for the close fitting sleeve material to provide a good shock impedance to the silicon carbide sample. The outer diameter of the sleeve was nominally 38 mm. The experimental configuration is shown schematically in Fig. 1.

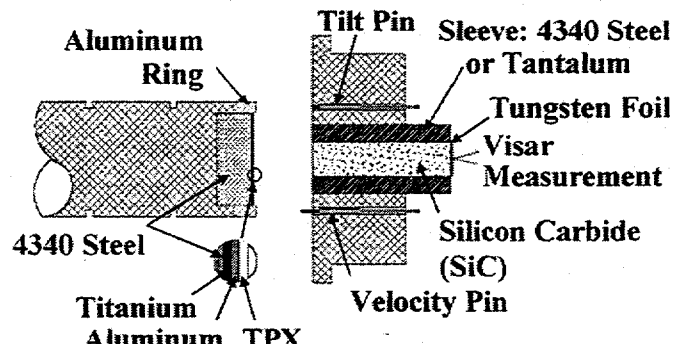


Figure 1. Experimental configuration of a layered impactor and a ceramic rod target assembly.

RECEIVED
 AUG 11 1999

OSTI

DISCLAIMER

This report was prepared as an account of work sponsored by an agency of the United States Government. Neither the United States Government nor any agency thereof, nor any of their employees, make any warranty, express or implied, or assumes any legal liability or responsibility for the accuracy, completeness, or usefulness of any information, apparatus, product, or process disclosed, or represents that its use would not infringe privately owned rights. Reference herein to any specific commercial product, process, or service by trade name, trademark, manufacturer, or otherwise does not necessarily constitute or imply its endorsement, recommendation, or favoring by the United States Government or any agency thereof. The views and opinions of authors expressed herein do not necessarily state or reflect those of the United States Government or any agency thereof.

DISCLAIMER

**Portions of this document may be illegible
in electronic image products. Images are
produced from the best available original
document.**

TABLE 1. Summary of impact experiments on silicon carbide

Test No.	Rod Length (mm)	Impactor Materials	Impactor Thickness (mm)	Impactor Velocity (km/s)	Sleeved
SiC1	74.506	Steel/Ti/Al/TPX	19.06/0.782/0.904/1.006	0.351	yes
SiC2	74.516	Steel/Ti/Al/TPX	19.07/0.775/0.927/1.006	0.484	yes
SiC3	74.813	Steel/Ti/Al/TPX	19.06/0.762/0.912/0.988	0.617	yes
SiC4	74.508	Steel/Ti/Al/TPX	19.05/0.767/0.909/1.006	0.396	yes
SiC5	74.933	Steel/Ti/Al/TPX	19.04/0.358/0.439/0.511	0.347	yes
SiC6	74.505	Steel/Ti/Al/TPX	19.07/0.356/0.439/0.508	0.506	yes
SiC7	76.276	Steel/Ti/Al/TPX	19.03/0.770/0.919/0.970	0.611	no
SiC8	75.753	Steel/Ti/Al/TPX	19.03/0.772/0.922/0.991	0.612	Yes (Ta)

The silicon carbide used in this study is referred to as Cercom SiC-B. Its composition consists of (99.3%) silicon carbide and is fabricated using hot pressed techniques. The density of the material used in this investigation was 3.217 g/cm³; the longitudinal and shear wave speed was determined to be 12.22 km/s and 7.75 km/s, respectively. This yields an estimate of 8.32 km/s, 11.81 km/s, and 0.164 for the bulk wave velocity, bar wave velocity, and Poisson's ratio, respectively. Specifically, this is the same batch of material used in previous studies on Cercom SiC. [8-10].

When unsleeved, a polyurethane foam was used to decouple the rod from the aluminum target fixture. A 0.055 mm thick tungsten reflector glued onto the free surface of the rod was used to obtain the axial particle velocity measurements using the velocity interferometer, VISAR having a time resolution of ~ 1 ns. The loading strain rate is varied either by varying the impact velocity or by varying the thickness of the layered impactors at the same impact velocity.

Effect of loading stress and loading rate

Four experiments were conducted with silicon carbide rods 74.5 mm in diameter and 19 mm in length with steel sleeves. The impact velocity was varied as shown in Table 1, causing the stress and the loading rate to vary at the impact interface. Fig. 2 shows the results of the experiments. The two experiments with lower impact velocity, SiC1 and SiC4, introduce stress levels that are below its Hugoniot elastic limit at the impact interface. The experiments SiC3 and SiC2 that exhibit a limiting maximum particle velocity, are those that introduce a stress at or beyond its Hugoniot Elastic limit. The

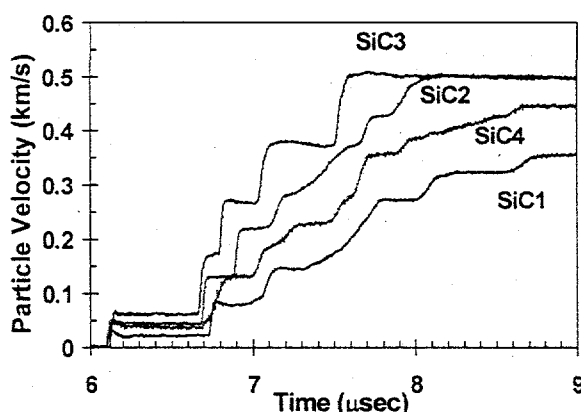


FIGURE 2. Effect of stress and loading rate results in higher peak particle velocity, until a maximum level is achieved.

overall effect of increasing stress and loading rate on steel-sleeved silicon carbide rod is that a higher peak particle velocity is achieved. The velocity can increase until the yield stress of silicon carbide is reached or exceeded at which time there is a limiting maximum particle velocity.

Effect of loading rate

A set of two experiments was performed to investigate the effects of loading rates at the same loading stress. This was accomplished by varying the dimensions of the layered impactor by approximately one half in SiC6 compared to those used in SiC2. The results are shown in Fig. 3. The experiment with the higher loading rate, SiC6, shows that it fails at a higher stress resulting in a higher peak particle velocity than the experiment with the lower loading rate, SiC2. A higher peak particle velocity implies a higher yield. This provides experimental evidence for the dependence of failure stress upon loading rate.

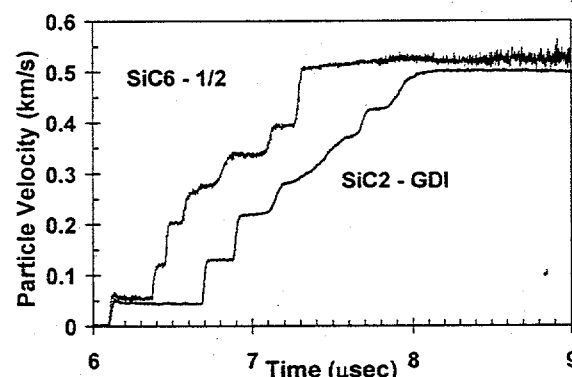


FIGURE 3. Effect of loading rate. Increasing loading rate results in higher peak particle velocity.

Effect of confinement

Three experiments were performed at the same impact velocity to determine the effect of varying confinement. A 4340 steel sleeve was used for SiC3, a tantalum sleeve was used for SiC8, and no sleeve was used for SiC7. These measurements are shown in Fig. 4. The peak particle velocity was lowest for the unsleeved silicon carbide, higher measured for the steel sleeved target and highest for the tantalum sleeved target. Measurements of higher peak particle velocity, for targets confined by materials of higher shock impedance

suggest the material can sustain a higher yield strength at a fairly higher stress.

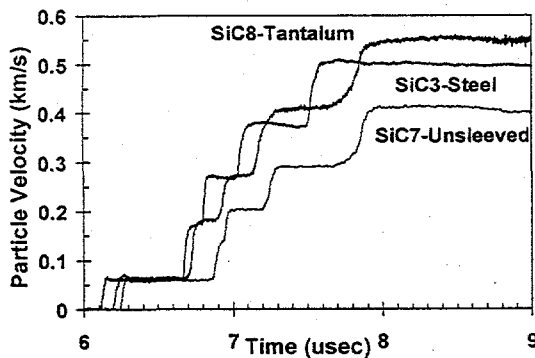


FIGURE 4. Effect of confinement. Confining SiC results in failure at higher stresses because more damage has occurred in the material.

3. Conclusions

Previous studies on impact of ceramic rods have concentrated upon using a single density impactor [11-13] to evaluate the uniaxial compressive behavior of the ceramics. However, due to the low spall strength of ceramics [8-9] the radial stress components will fracture the material during the loading phase even though the mean stress of the material indicates compression [4]. The technique proposed herein (i.e., using graded-density impactors to study the uniaxial compressive behavior of the rods) circumvents this problem by reducing the magnitude of tension generated in silicon carbide during loading [4]. A sleeved rod prevents the formation of radial tension during the loading process [4]. It is not surprising therefore that the bare rod (SiC 7) yields a failure stress of 7.8 GPa, the steel-sleeved rod (SiC3) 9.7 GPa, and the tantalum-sleeved rod (SiC8) 10.66 GPa. The material that is damaged the most (SiC7) fails at a lower stress. It is anticipated that SiC7 will be damaged the most mainly because the radial stress components exhibit tension states.

The current experiments address strain rate effects in SiC at strain rates of $\sim 10^4$ /s. This strain-rate regime is difficult to access either by Hopkinson bar techniques or shock loading techniques. The leading edge of the axial compression wave traverses at an elastic wave speed (12.2 km/s), followed by a second compression wave traveling at a bar wave speed loading the material to a final stress at a strain rate of $\sim 10^4$ /s. The first compression state σ_1 is calculated using $\sigma_1 = (\rho_0 c_1 \delta u_f)/2$, where ρ_0 is the initial density, c_1 the elastic wave speed, and δu_f the incremental free surface velocity measurement associated with the longitudinal elastic wave. The axial compression state σ_a and the loading strain rates ε associated with the bar wave are calculated using $\sigma_a = (\rho_0 c_b \Delta u_f)/2$ and $\varepsilon = \Delta u_f/(2c_b t)$, where c_b is the bar wave velocity, and Δu_f the corresponding free-surface velocity measurement, and t the time duration for loading. Results of these experiments are shown in Figure 5, and are compared to the low strain-rate Hopkinson bar experiments at strain-rates $\leq 10^3$ /s [14]. The low strain-rate experiments yield a failure stress of ~ 4 GPa and shows evidence of an increase to ~ 6 GPa at strain rates slightly above 10^3 /s [14]. As the strain rate varies from 7.5×10^3 /s to 1.8×10^4 /s in these studies, the

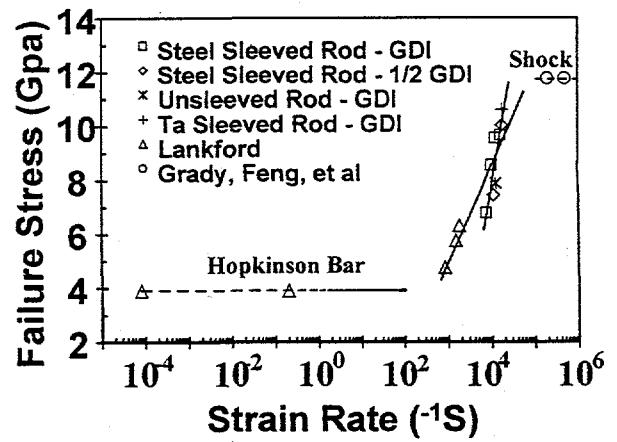


FIGURE 5. Failure stress of SiC as a function of loading rate.

corresponding failure stress varies from ~ 6.7 GPa to 10.6 GPa. The results clearly indicate the dependence of the failure stress on the loading rates and seen to transition to higher estimates of strength determinations obtained from shock experiments, and are consistent with those obtained for coors AD995 alumina (see Figure 6). The results lead credence to the hypothesis that damage kinetics is rate-dependent, and ultimately, shock experiments yield higher estimates of strength because rate-dependent kinetics prevent the nucleation and growth of flaws/defects in materials during rapid loading.

CTH-calculational results [4] indicate that the ratio of the lateral stress to the axial stress is ~ 0.23 for the single-density impact of the alumina rod, and ~ 0.1 and ~ 0.08 for the graded-density impact of the unsleeved and sleeved rod, respectively. This apparently indicates that the degree of confinement is least for the sleeved rod. This is consistent with the earlier inference that the stress propagation in the rods transitions to a uniaxial stress motion when it is loaded at finite rates, and is shown in Figure 7. Therefore, the experimental measurements of a higher failure stress (5.1 GPa) for the sleeved-alumina rod when compared to the lowest value (3.4 GPa) are not due to the sleeved-confinement of the rod, but are more related to strain-rate sensitivities. This is indicated in Figure 6. This is also true for silicon carbide as indicated in Figure 5.

The most significant result of this study is that the use of a graded-density impactor in combination with sleeved rods allows accessibility to intermediate strain rates. Current results for SiC and previous studies on alumina [4-5] both suggest that the failure stress of ceramics is strain-rate-dependent. It appears that loading rates of a few times 10^4 /s can be achieved by optimizing the design of the graded density layered materials, the diameter of the bar, and the impact velocity. Concepts are currently being pursued to achieve yet higher loading rates of 10^5 /s. One approach under consideration is to use the graded-density materials as an impactor to perform isentropic loading experiments up to its Hugoniot elastic limit. This will achieve lower loading rates than those obtained in single shock experiments.

References

1. L. C. Chhabildas, and R. A. Graham, in *Techniques and Theory of Stress Measurements for Shock Wave*

- Applications*, 83, Edited by R. B. Stout, et. al., AMD, 1987 pp. 1-18.

 2. L. C. Chhabildas, L. N. Kmetyk, W. D. Reinhart, and C. A. Hall, *Int. J. Impact Engng.* 17 (1995) pp. 183-194.
 3. L. C. Chhabildas, J. E. Dunn, W. D. Reinhart, and J. M. Miller, *Int. J. Impact Engng.* 14 (1993) pp. 121-132.
 4. L. C. Chhabildas, M. D. Furnish, D. E. Grady, *Proceedings of the DYMAT International Conference on Mechanical and Physical behavior of Materials*, 1997.
 5. L. C. Chhabildas, M. D. Furnish, W. D. Reinhart, D. E. Grady in *Shock Compression of Condensed Matter-1997*, edited by S. C. Schmidt, D. P. Dandekar, and J. W. Forbes, New York, AIP Press, 1998, pp. 505-508.
 6. K. G. Holland, L. C. Chhabildas, W. D. Reinhart, M. D. Furnish, Experiments of Cercom SiC Rods under Impact, in *Shock Compression of Condensed Matter-1999*, edited by M. D. Furnish, L. C. Chhabildas, and R. S. Hixson, New York, AIP Press, 2000 (to be published).
 7. L. M. Barker and R. E. Hollenbach, *J. Appl. Phys.* 43, (1972), pp. 4669-4675.
 8. D. E. Grady, Sandia National Laboratories Report, SAND94-3266, February 1995.
 9. P. Bartkowski, and D. P. Dandekar, in *Shock Compression of Condensed Matter-1995*, edited by Schmidt, S. C. and Tao, W. C., New York, AIP Press, 1996, pp. 535-538.
 10. R. Feng, G. F. Raiser, and Y. M. Gupta, *J. Appl. Phys.*, 83, 1998
 11. A. Cosculluela, J. Cagnoux, F. Collombet, *Journal de Physique IV*, C3 (1991) pp. 109-116.
 12. N. S. Brar, and S. J. Bless in *Shock-Wave and High-Strain-Rate Phenomena in Materials*, Edited by M. A. Meyers et. al., 1992, pp. 1041-1049.
 13. J. L. Wise, D. E. Grady, *High Pressure Science and Technology-1993*, AIP Conference Proceeding 309, Edited by S. C. Schmidt et. al., 1994, pp. 733-736.
 14. J. Lankford, J. Amer. Ceramic Soc., 64, C33-C34 (1981).

shown.

Figure 7. Variation of calculated failure stress as a function of confinement *i.e.*, the ratio of lateral stress to axial stress.

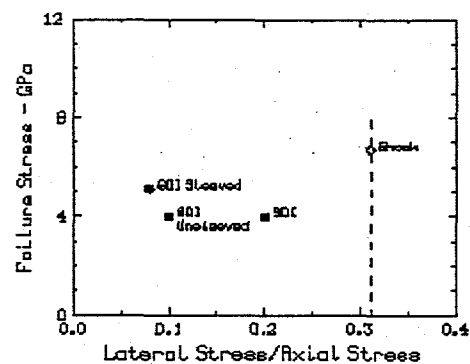


Figure 6. Variation of failure stress with strain rate for Coors AD995. Quasi-static and shock loading experiments are also

